studies revealed that this is a kinetic effect, and both solvents work well at slightly elevated temperature starting from around 40 °C [39]. Increasing the cell temperature can also promote side reactions that started when exceeding temperatures of 70–80 °C.

1.4.4 Physicochemical Properties

For battery electrolytes, two of the more important physicochemical properties are viscosity and ionic conductivity, and both properties are highly dependent on temperature. For glymes, the viscosity increases with the length of the glyme from 0.78 mPas (monoglyme) to 7.59 mPas (tetraglyme) at 20 °C. For monoglyme, the viscosity was only determined at 20 °C due to the high vapor pressure. The viscosity, however, for pentaglyme is much greater than the other glymes, with 186 mPas at 20 °C, but once the temperature is increased, the viscosity decreases sharply to 72.2 mPas (50 °C) all the way down to 22.4 mPas (80 °C). Although kinetic properties of electrode reactions depend on many parameters, low values of viscosity are favored [39]. The ionic conductivity of the electrolyte is critical for the battery. The diglyme-based electrolyte has a significantly higher conductivity than electrolytes based on mono-, tri-, tetra-, and pentaglyme and crown ethers. Using NaOTf, the ionic conductivity in diglyme is 4.47 mS cm^{-1} at 20 °C and increases to 5.91 mS cm^{-1} at 60 °C and 6.23 mS cm^{-1} at 80 °C, even at −30 °C, the conductivity is 1.59 mS cm^{-1}. The low freezing point of diglyme (−64 °C) is an advantage in view of low temperature battery operation. It is worth to mention that the ionic conductivity of triglyme-based electrolyte is particularly low at 20 °C, only having an ionic conductivity of 0.306 mS cm^{-1}; however, it quickly rises to 2.60 mS cm^{-1} at 60 °C all the way to 3.56 mS cm^{-1} at 80 °C [39]. Again, this might be connected with the unfavorable coordination between triglyme and the sodium ion [29e, 39].

Several Raman spectroscopy studies have shown how the G, D, and D′ bands are affected by the co-intercalation process [31b, 32, 41a, 51]. Pristine graphite displays a strong G band and a weak D band, characteristic of the strong sp^2-hybridized C—C bonds. Upon co-intercalation the intensity of the D band increases greatly, and the D′ band emerges, indicating sp^3 defects and the formation of a staged GIC, as shown in Figure 1.6 [31b, 41a, 51]. The excellent cyclability is again manifested by the Raman measurements, as barely any changes in the structure are observed over 8000 cycles [32].

Besides showing an impressive capacity retention of 96% after 8000 cycles and the ability to operate at 65% of capacity at a current density of 30 A g^{-1}, i.e. the cell can be fully charged in 12.5 seconds, Cohn et al. investigated the diffusion of solvated sodium ions using the galvanostatic intermittent cycling technique and attributed the great rate capabilities to the fast diffusion of the sodium ions in the electrode material [32]. Similarly, Jung et al. made theoretical investigations of the diffusion of solvated sodium ions between the graphene layers and found, surprisingly, that the diffusion coefficients were an order of magnitude higher for the solvated sodium ions compared with bare sodium or lithium ions, i.e. *t*-GICs might be especially suited for high-power batteries [35c].

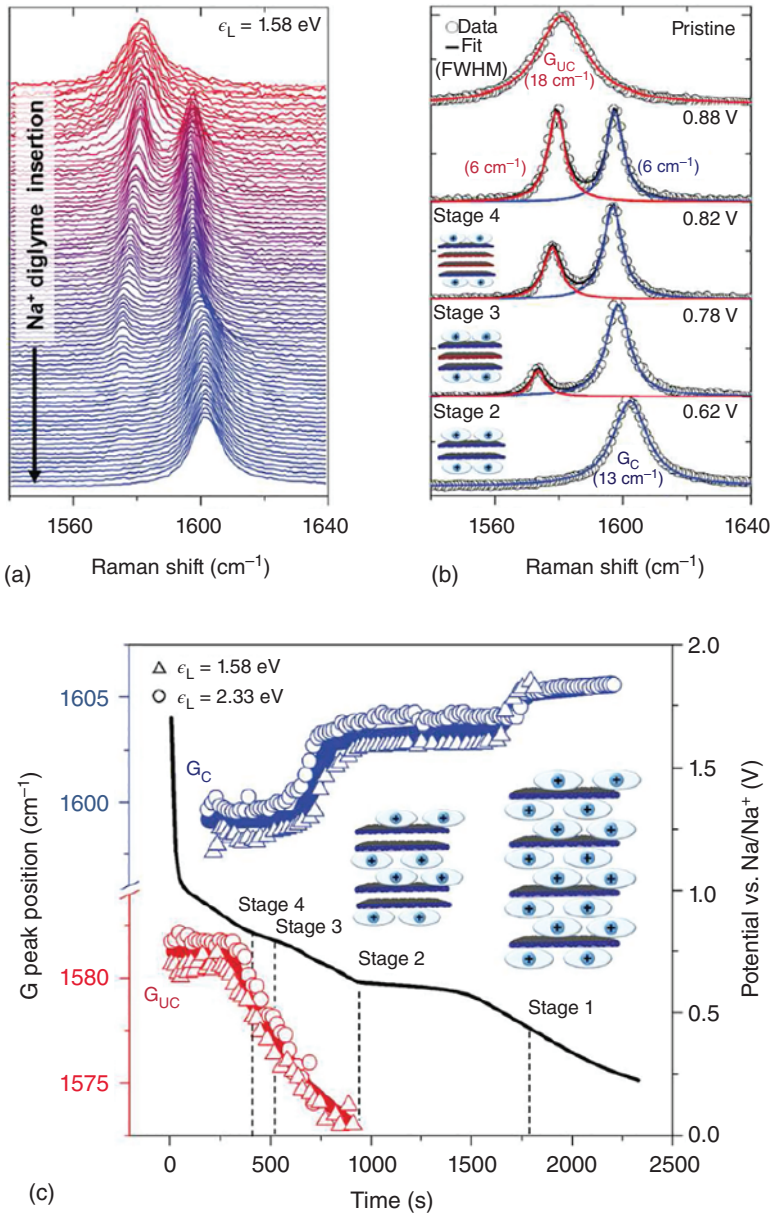

Figure 1.6 (a) In situ Raman spectra showing the highly ordered staging reaction with (b) selected spectra and Lorentzian fits of components. (c) Tracking the positions of the Raman G peak components during the electrochemical intercalation reaction with the corresponding Galvanostatic discharge (~0.2 A g^{-1}) profile shown with respect to right *y*-axis (black line). Source: From [32]/with permission of American Chemical Society.

1.4.5 Solid Electrolyte Interphase (SEI)

The SEI has been thoroughly studied for LIBs. The SEI directly affects the battery performance, and its formation and characteristics are hence of great importance. Ideally, the SEI is electronically insulating, ionically conducting, chemically and mechanically stable (but flexible enough to follow the volume changes during cycling), and it should form within the initial cycles such that the system quickly stabilizes [52]. From a classical perspective, the SEI also prevents any solvent co-intercalation. Without doubt, a reversible graphite electrode based on solvent co-intercalation questions this traditional concept of an SEI. Whether or not an SEI exists in the case of reversible *t*-GICs electrodes is therefore controversially discussed. Especially, the fact that the reaction can be so fast indicates an extremely low charge transfer resistance for the solvated Na^+, which, at the same time, would require an SEI-free (or nearly SEI-free) interface. Several studies therefore addressed the characteristics of the SEI. While Maibach et al. [52] and Wang et al. [53] reported on an existing SEI, our group and the Kang group concluded that the co-intercalation reaction requires an "SEI-free" interface that was supported by transmission electron microscopy (TEM), X-ray photoelectron spectroscopy (XPS), and Online electrochemical mass spectroscopy (OEMS) studies [45, 54]. None of the analytical tools is perfect, and analyzing SEIs on battery electrodes is chronically difficult for various reasons. In some cases, however, the different findings can be explained by different experimental conditions. Wang et al. used a graphite electrode with a large fraction of super-P as additive, and the studies by Maibach et al. and Goktas et al. used different electrolytes (NaFSI in tetraglyme vs. NaOTf in diglyme). Our own findings indicate that NaFSI causes additional side reactions [48] that may artificially lead to an excessive SEI formation. Moreover, an SEI may also form on conductive additives that may mask the graphite particles. A similar problem arises from the binder that is typically used to prepare electrodes. An indication of excessive side reactions can be seen from the Coulomb efficiencies that are low for the electrodes with large amounts of conductive additive and NaFSI-containing electrolytes.

Figure 1.7 shows TEM images of graphite particles after electrochemical cycling. The left image shows the results for a Li cell with carbonate electrolyte (*b*-GIC formation) for which an SEI can be observed. The right image shows results for a Na cell after cycling in a diglyme electrolyte (*t*-GIC formation). When cycling this electrode, neither binder nor conductive additive was used. In this case, an SEI is not visible. Similar results were reported by Kim et al. who could not find an SEI by TEM (and XPS) [54]. As mentioned, analysis is challenging and the common techniques to study the SEI such as XPS and TEM are postmortem techniques that require a sample transfer and sample preparation that may cause surface reactions that may be misinterpreted as an SEI. On the other hand, too intense washing of the electrodes during sample preparation may wash off the SEI. Moreover, contamination of the graphite surface may also arise from reactions of the electrolyte with the counter electrode (cross-talk).

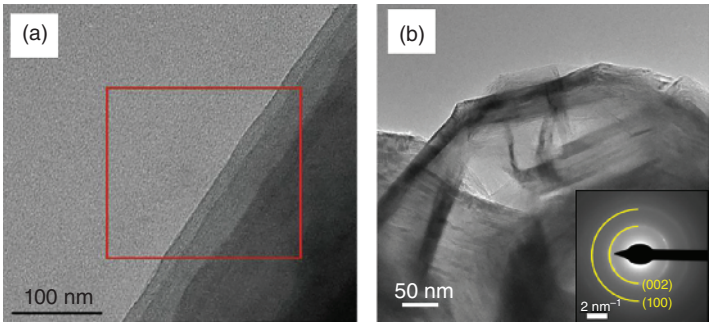

Figure 1.7 (a) TEM images of fresh graphite and SEI on graphite anodes cycled to four cutoff voltages in 1.2 M $LiPF_6$/EC during first charge (Source: From [55]/with permission of American Chemical Society); (b) TEM and HRTEM images of the graphite particles after cycling in electrolyte solutions of 1 M NaOTf in diglyme (end of fifth cycle, desodiated state). Insets: Selected area electron diffraction (SAEDs) patterns for areas; the semi-circles indicate the expected positions for graphite interplanar distances. (Source: From [48]/with permission of American Chemical Society).

Overall, the charge transfer of solvated ions into graphite is quite intriguing. Whether or not an SEI exists in case of reversible *t*-GIC formation remains a matter of debate. Related to that, theoretical studies suggest that diglyme can be indeed stable at low potentials that may prevent SEI formation [56].

1.4.6 Increasing the Capacity

A major limitation of using graphite as electrode in SIBs is the limited capacity, which still remains at around 110 mAh g^{-1} for the *t*-GIC formation. This value is low for battery electrodes (should be $\gg$150 mAh g^{-1}) but high compared to capacitive electrodes, which indicates that *t*-GIC formation may be more suited to design high-power electrodes, e.g. also for hybrid capacitors. A higher capacity could be obtained by finding new Na *t*-GICs in which more sodium can be stored. The attempts so far, however, were not successful. A more practical approach to increase the capacity is to add metals. For LIBs, it is well known that small amounts of silicon can be added to graphite electrodes in order to increase the capacity. The general downside of high-capacity metals such as Si or Sn is that they show an extremely large volume expansion/shrinkage that leads to poor cycle life, so a careful optimization of the electrode and metal content is required. Si so far does not show good properties as anode in SIBs, but promising results were obtained for Sn that shows a theoretical capacity of 847 mAh g^{-1} for the formation of $Na_{3.75}Sn$ [57]. The theoretical volume expansion of Sn during complete sodiation is around 430% [58]. But for a carbon/Sn composite, the expansion on the electrode level can be much smaller. For example, Palaniselvam et al. found an expansion of 14% for a composite containing 58 wt% Sn and 42 wt% hard carbon [59]. Our group therefore also added small amounts of Sn to a graphite electrode and studied the impact on the Na storage behavior [43]. For an electrode containing 17 wt% Sn and 83 wt% graphite, the capacity reached 223 mAh g^{-1}, i.e. roughly doubling the

capacity compared to the pure graphite electrode. The ICE remained high at 90%, and the electrode showed a high-capacity retention for at least 2200 cycles. While the additional tin doubles the capacity, its contribution to the electrode expansion is negligible (~3%). Due to the high rate capability of the reaction, the electrode was tested as anode in a Na-ion hybrid capacitor (with an activated carbon as cathode). Excellent long-term cyclability with 80% of the original capacity after 8000 cycles were obtained. Based on the mass of the electrodes, the cell delivered an energy density 93 Wh kg^{-1} of and a power density of 7.8 kW kg^{-1}.

1.5 Outlook

Even though the formation of sodium-glyme *t*-GICs has gathered attention in the past few years, several questions are still left open for future research. First of all, the fundamental question of what combination of properties of the solvents, ions, and electrode material that enable these highly reversible co-intercalation and charge transfer processes remains unanswered and largely unaddressed. The desolvation energy, however, has been identified as a critical quantity, but a very limited set of solvents have been investigated in this regard [35d]. In fact, as the exact stoichiometry of the co-intercalation process in glyme-based electrolytes and graphite is unknown, more thorough and detailed investigations are probably needed before a fundamental understanding of the phenomenon can be established. Once such an understanding is achieved, it is possible that several new systems operating by the co-intercalation mechanism can be found; in fact, there are several studies on using potassium and di- or even trivalent cations [34].

Several studies have argued, or asserted, that a single diglyme molecule is brought along the sodium ion, and thus partial desolvation occurs before the ion enters the active material [28b, 35a, c, d]. For instance, one study measured the mass change of the graphite electrode along with energy dispersive X-ray spectroscopy and found that there is one solvent per cation [35a], and several theoretical studies have looked at a single solvent around the sodium ion [35b, 45]. Similarly, several studies have argued or, again, asserted, that two diglyme solvents are brought along the sodium ion, and hence no desolvation occurs in the charge transfer process, and theoretical studies have seen excellent agreement between the XRD measured graphene layer spacing and the computed spacing when the sodium ion is solvated by two diglymes [35b, 37, 45]. Two NMR studies found that the solvation shell remains intact with two diglyme molecules around the sodium ion in the graphite host, along with additional free diglyme molecules [35b, 37]. Moreover, one of the NMR studies revealed that the sodium solvation shells interact more weakly with the graphite than the lithium counterparts, allowing for faster diffusion of sodium ions [37]. Needless to say, as the research community is divided on what exactly enters the graphite galleries, more research is needed before the question can be settled.

As stated previously, several studies have investigated the SEI in these systems, but the results remain inconclusive, possibly due to the studied systems not being identical, and thus the existence, and, if so, the characteristics of the SEI

is still left unanswered. But, it is clear that the great rate capabilities cannot be achieved without the interface being highly permeable for entire solvation shells. Practical questions to be addressed in the future also relate to realistic full cells with minimized electrolyte volume and multilayers where the large breathing may lead to mechanical problems. It is therefore especially desirable to find Na-rich *t*-GICs with higher capacity but at the same time smaller lattice expansion. A more rational development would be enabled by a better understanding of the complex interactions between the graphite lattice, the Na ions, and the co-intercalated solvent molecules. A key advantage of Na *t*-GICs for practical applications so far seems the fast in-plane diffusion that could enable high-power devices.

References

1 (a) (1990). *Graphite Intercalation Compounds I*. Berlin: Springer-Verlag. (b) Inagaki, M. (1989). Applications of graphite intercalation compounds. *Journal of Materials Research* 4: 1560–1568. (c) Li, Y., Lu, Y., Adelhelm, P. et al. (2019). Intercalation chemistry of graphite: alkali metal ions and beyond. *Chemical Society Reviews* 48: 4655–4687. (d) Hérold, C. and Lagrange, P. (2006). Intercalation reactions into graphite: a two-dimensional chemistry; Les reactions d'intercalation dans le graphite. Une chimie bidimensionnelle. *Actualite Chimique* 33–37. (e) Zhang, M., Song, X., Ou, X., and Tang, Y. (2019). Rechargeable batteries based on anion intercalation graphite cathodes. *Energy Storage Materials* 16: 65–84. (f) Placke, T., Heckmann, A., Schmuch, R. et al. (2018). Perspective on performance, cost, and technical challenges for practical dual-ion batteries. *Joule* 2: 2528–2550. (g) Xu, J., Dou, Y., Wei, Z. et al. (2017). Recent progress in graphite intercalation compounds for rechargeable metal (Li, Na, K, Al)-ion batteries. *Advanced Science* 4: 1700146.

2 (a) Salvatore, M., Carotenuto, G., De Nicola, S. et al. (2017). Synthesis and characterization of highly intercalated graphite bisulfate. *Nanoscale Research Letters* 12: 167. (b) Rüdorff, W. (1959). Graphite intercalation compounds. *Advances in Inorganic Chemistry and Radiochemistry* 1: 223–266.

3 Yazami, R. and Touzain, P. (1983). A reversible graphite-lithium negative electrode for electrochemical generators. *Journal of Power Sources* 9: 365–371.

4 Schafhäutl, C. (1840). *Journal für praktische Chemie* 21: 129–157.

5 Brodie, B. (1855). *Annals de Chemie et de Physique* 45: 351–352.

6 Rüdorff, W. and Hofmann, U. (1938). *Zeitschrift für anorganische und allgemeine Chemie* 238: 1–50.

7 (a) Guerard, D. and Herold, A. (1975). Intercalation of lithium into graphite and other carbons. *Carbon* 13: 337–345. (b) Sole, C., Drewett, N.E., and Hardwick, L.J. (2014). In situ Raman study of lithium-ion intercalation into microcrystalline graphite. *Faraday Discussions* 172: 223–237. (c) Winter, M., Besenhard, J.O., Spahr, M.E., and Novák, P. (1998). Insertion electrode materials for rechargeable lithium batteries. *Advanced Materials* 10: 725–763. (d) Senyshyn, A., Dolotko, O., Mühlbauer, M.J. et al. (2013). Lithium intercalation into graphitic carbons

revisited: experimental evidence for twisted bilayer behavior. *Journal of The Electrochemical Society* 160: A3198–A3205. (e) Schweidler, S., de Biasi, L., Schiele, A. et al. (2018). Volume changes of graphite anodes revisited: a combined operando x-ray diffraction and in situ pressure analysis study. *The Journal of Physical Chemistry C* 122: 8829–8835.

8 Daumas, N. and Herold, A. (1969). *Comptes Rendus des Seances de l'Academie des Sciences, Serie C. Sciences Chimiques*.

9 (a) Gavilán-Arriazu, E.M., Pinto, O.A., López de Mishima, B.A. et al. (2018). The kinetic origin of the Daumas-Herold model for the Li-ion/graphite intercalation system. *Electrochemistry Communications* 93: 133–137. (b) Krishnan, S., Brenet, G., Machado-Charry, E. et al. (2013). Revisiting the domain model for lithium intercalated graphite. *Applied Physics Letters* 103: 251904. (c) Mathiesen, J.K., Johnsen, R.E., Blennow, A.S., and Norby, P. (2019). Understanding the structural changes in lithiated graphite through high-resolution operando powder X-ray diffraction. *Carbon* 153: 347–354.

10 Dimiev, A.M., Shukhina, K., Behabtu, N. et al. (2019). Stage transitions in graphite intercalation compounds: role of the graphite structure. *The Journal of Physical Chemistry C* 123: 19246–19253.

11 (a) Brandt, N.B., Chudinov, S.M., and Ponomarev, Y.G. (1988). *Modern Problems in Condensed Matter Sciences*,Chapter 10, vol. 20, 197–321. Elsevier. (b) Dresselhaus, M.S. and Dresselhaus, G. (2002). *Advances in Physics* 51: 1–186.

12 Zabel, H. and Solin, S. (1990). *Graphite Intercalation Compounds I, Structure and Dynamics*, vol. 14. Springer Series in Materials Science.

13 (a) Nayak, P.K., Yang, L., Brehm, W., and Adelhelm, P. (2018). From lithium-ion to sodium-ion batteries: advantages, challenges, and surprises. *Angewandte Chemie International Edition* 57: 102–120. (b) Hosaka, T., Kubota, K., Hameed, A.S., and Komaba, S. (2020). Research development on K-ion batteries. *Chemical Reviews* 120: 6358–6466.

14 (a) Das, S.K., Mahapatra, S., and Lahan, H. (2017). Aluminium-ion batteries: developments and challenges. *Journal of Materials Chemistry A* 5: 6347–6367. (b) Elia, G.A., Marquardt, K., Hoeppner, K. et al. (2016). An overview and future perspectives of aluminium batteries. *Advanced Materials* 28: 7564–7579.

15 Sui, Y., Liu, C., Masse, R.C. et al. (2020). Dual-ion batteries: the emerging alternative rechargeable batteries. *Energy Storage Materials* 25: 1–32.

16 Fauchard, M., Cahen, S., Lagrange, P. et al. (2019). Overview on the intercalation of gold into graphite. *Carbon* 145: 501–506.

17 Zhang, C., Ma, J., Han, F. et al. (2018). Strong anchoring effect of ferricchloride-graphite intercalation compounds (FeCl 3-GICs) with tailored epoxy groups for high-capacity and stable lithium storage. *Journal of Materials Chemistry A* 6: 17982–17993.

18 Li, Z., Zhang, C., Han, F. et al. (2020). Towards high-volumetric performance of Na/Li-ion batteries: a better anode material with molybdenumpentachloride–graphite intercalation compounds (MoCl5-GICs). *Journal of Materials Chemistry A* 8: 2430–2438.

19 Solin, S.A. (1986). Ternary graphite intercalation compounds. In: *Intercalation Layered Materials* (ed. M.S. Dresselhaus), 291–300. Springer.

20 (a) Blomgren, G.E. (2016). The development and future of lithium ion batteries. *Journal of The Electrochemical Society* 164: A5019–A5025. (b) Yoshino, A., Sanechika, K., and Nakajima, T. (1987). US Patent 4,668,595A.

21 Stevens, D.A. and Dahn, J.R. (2001). The mechanisms of lithium and sodium insertion in carbon materials. *Journal of The Electrochemical Society* 148: A803.

22 (a) Yabuuchi, N., Kubota, K., Dahbi, M., and Komaba, S. (2014). Research development on sodium-ion batteries. *Chemical Reviews* 114: 11636–11682. (b) Irisarri, E., Ponrouch, A., and Palacin, M.R. (2015). Hard carbon negative electrode materials for sodium-ion batteries. *Journal of The Electrochemical Society* 162: A2476–A2482. (c) Dou, X., Hasa, I., Saurel, D. et al. (2019). Hard carbons for sodium-ion batteries: structure, analysis, sustainability, and electrochemistry. *Materials Today* 23: 87–104. (d) Xie, F., Xu, Z., Guo, Z., and Titirici, M.-M. (2020). Hard carbons for sodium-ion batteries and beyond. *Progress in Energy* 2: 042002.

23 (a) Dahn, J.R. (1991). Phase diagram of LixC6. *Physical Review B: Condensed Matter* 44: 9170–9177. (b) Ohzuku, T., Iwakoshi, Y., and Sawai, K. (1993). Formation of lithium-graphite intercalation compounds in nonaqueous electrolytes and their application as a negative electrode for a lithium ion (shuttlecock) cell. *Journal of The Electrochemical Society* 140: 2490–2498.

24 (a) Charlier, A., Charlier, M.F., and Fristot, D. (1989). Binary graphite intercalation compounds. *Journal of Physics and Chemistry of Solids* 50: 987–996. (b) Nobuhara, K., Nakayama, H., Nose, M. et al. (2013). First-principles study of alkalimetal-graphite intercalation compounds. *Journal of Power Sources* 243: 585–587.

25 (a) Fong, R., Sacken, U.Y., and Dahn, J.R. (1990). Studies of lithium intercalation into carbons using nonaqueous electrochemical cells. *Journal of The Electrochemical Society* 137: 2009–2013. (b) Dey, A.N. and Sullivan, B.P. (1970). The electrochemical decomposition of propylene carbonate on graphite. *Journal of Electrochemical Society* 117: 222–224.

26 (a) Xu, K. (2019). A long journey of lithium: from the big bang to our smartphones. *Energy & Environmental Materials* 2: 229–233. (b) Winter, M., Barnett, B., and Xu, K. (2018). Before Li ion batteries. *Chemical Reviews* 118: 11433–11456.

27 (a) Peled, E. (1979). The electrochemical behavior of alkali and alkaline earth metals in nonaqueous battery systems—the solid electrolyte interphase model. *Journal of The Electrochemical Society* 126: 2047. (b) Peled, E., Golodnitsky, D., and Ardel, G. (1997). Advanced model for solid electrolyte interphase electrodes in liquid and polymer electrolytes. *Journal of Electrochemical Society* 144: L208–L210. (c) Peled, E. and Menkin, S. (2017). SEI: past, present and future. *Journal of The Electrochemical Society* 164: A1703–A1719.

28 (a) Krauskopf, T., Richter, F.H., Zeier, W.G., and Janek, J. (2020). Physicochemical concepts of the lithium metal anode in solid-state batteries. *Chemical Reviews* 120: 7745–7794. (b) Fang, C., Wang, X., and Meng, Y.S. (2019). Key issues

hindering a practical lithium-metal anode. *Trends in Chemistry* 1: 152–158. (c) Zhang, X.-Q., Cheng, X.-B., and Zhang, Q. (2018). Advances in interfaces between Li metal anode and electrolyte. *Advanced Materials Interfaces* 5: 1701097. (d) Li, S., Jiang, M., Xie, Y. et al. (2018). Developing high-performance lithium metal anode in liquid electrolytes: challenges and progress. *Advanced Materials* 30: 1706375. (e) Yu, X. and Manthiram, A. (2018). Electrode-electrolyte interfaces in lithium-based batteries. *Energy & Environmental Science* 11: 527–543. (f) Nair, J.R., Imholt, L., Brunklaus, G., and Winter, M. (2019). Lithium metal polymer electrolyte batteries: opportunities and challenges. *The Electrochemical Society Interface* 28: 55–61.

29 (a) Wenzel, S., Hara, T., Janek, J., and Adelhelm, P. (2011). Room-temperature sodium-ion batteries: Improving the rate capability of carbon anode materials by templating strategies. *Energy & Environmental Science* 4: 3342. (b) Slater, M.D., Kim, D., Lee, E., and Johnson, C.S. (2013). Sodium-ion batteries. *Advanced Functional Materials* 23: 947–958. (c) Ge, P. and Fouletier, M. (1988). Electrochemical intercalation of sodium in graphite. *Solid State Ionics* 28–30: 1172–1175. (d) Cabello, M., Chyrka, T., Klee, R. et al. (2017). Treasure Na-ion anode from trash coke by adept electrolyte selection. *Journal of Power Sources* 347: 127–135. (e) Jache, B., Binder, J.O., Abe, T., and Adelhelm, P. (2016). A comparative study on the impact of different glymes and their derivatives as electrolyte solvents for graphite co-intercalation electrodes in lithium-ion and sodium-ion batteries. *Physical Chemistry Chemical Physics* 18: 14299–14316.

30 (a) Liu, Y., Merinov, B.V., and Goddard, W.A. 3rd, (2016). Origin of low sodium capacity in graphite and generally weak substrate binding of Na and Mg among alkali and alkaline earth metals. *Proceedings of the National Academy of Sciences* 113: 3735–3539. (b) Moriwake, H., Kuwabara, A., Fisher, C.A.J., and Ikuhara, Y. (2017). Why is sodium-intercalated graphite unstable? *RSC Advances* 7: 36550–36554. (c) Lenchuk, O., Adelhelm, P., and Mollenhauer, D. (2019). New insights into the origin of unstable sodium graphite intercalation compounds. *Physical Chemistry Chemical Physics* 21: 19378–19390. (d) Wang, Z., Selbach, S.M., and Grande, T. (2014). Van der Waals density functional study of the energetics of alkali metal intercalation in graphite. *RSC Advances* 4: 4069–4079.

31 (a) Jache, B. and Adelhelm, P. (2014). Use of graphite as a highly reversible electrode with superior cycle life for sodium-ion batteries by making use of co-intercalation phenomena. *Angewandte Chemie International Edition* 53: 10169–10173. (b) Kim, H., Hong, J., Park, Y.-U. et al. (2015). Sodium storage behavior in natural graphite using ether-based electrolyte systems. *Advanced Functional Materials* 25: 534–541.

32 Cohn, A.P., Share, K., Carter, R. et al. (2016). Ultrafast solvent-assisted sodium ion intercalation into highly crystalline few-layered graphene. *Nano Lett* 16: 543–548.

33 (a) Solin, S.A. and Zabel, H. (1988). The physics of ternary graphite intercalation compounds. *Advances in Physics* 37: 87–254. (b) Lagrange, P., Bendriss-Rerhrhaye, A., and Mcrae, J.F.M.A.E. (1985). Synthesis and electrical

properties of some new ternary graphite intercalation compounds. *Synthetic Metals* 12: 201–206.

34 Park, J., Xu, Z.-L., and Kang, K. (2020). Solvated ion intercalation in graphite: sodium and beyond. *Frontiers in Chemistry* 8: 432–432.

35 (a) Kim, H., Hong, J., Yoon, G. et al. (2015). Sodium intercalation chemistry in graphite. *Energy & Environmental Science* 8: 2963–2969. (b) Gotoh, K., Maruyama, H., Miyatou, T. et al. (2016). Structure and dynamic behavior of sodium–diglyme complex in the graphite anode of sodium ion battery by 2H nuclear magnetic resonance. *The Journal of Physical Chemistry C* 120: 28152–28156. (c) Jung, S.C., Kang, Y.J., and Han, Y.K. (2017). Origin of excellent rate and cycle performance of Na±solvent cointercalated graphite vs. poor performance of Li±solvent case. *Nano Energy* 34: 456–462. (d) Yoon, G., Kim, H., Park, I., and Kang, K. (2016). Conditions for reversible Na intercalation in graphite: theoretical studies on the interplay among questions, solvent, and graphite host. *Advanced Energy Materials* 1601519. (e) Kim, H., Yoon, G., Lim, K., and Kang, K. (2016). A comparative study of graphite electrodes using the co-intercalation phenomenon for rechargeable Li, Na and K batteries. *Chemical Communiations* 52: 12618–12621.

36 Seidl, L., Bucher, N., Chu, E. et al. (2017). Intercalation of solvated Na-ions into graphite. *Energy & Environmental Science* 10.

37 Leifer, N., Greenstein, M.F., Mor, A. et al. (2018). NMR-detected dynamics of sodium co-intercalation with diglyme solvent molecules in graphite anodes linked to prolonged cycling. *The Journal of Physical Chemistry C* 122: 21172–21184.

38 Gotoh, K. (2021). ^{23}Na solid-state NMR analyses for Na-ion batteries and materials. *Batteries & Supercaps* 4: 1267–1278.

39 Goktas, M., Akduman, B., Huang, P. et al. (2018). Temperature-induced activation of graphite co-intercalation reactions for glymes and crown ethers in sodium-ion batteries. *The Journal of Physical Chemistry C* 122: 26816–26824.

40 Xu, Z.-L., Yoon, G., Park, K.-Y. et al. (2019). Tailoring sodium intercalation in graphite for high energy and power sodium ion batteries. *Nature Communications* 10: 2598.

41 Zhu, Z., Cheng, F., Hu, Z. et al. (2015). Highly stable and ultrafast electrode reaction of graphite for sodium ion batteries. *Journal of Power Sources* 293: 626–634.

42 Hasa, I., Dou, X., Buchholz, D. et al. (2016). A sodium-ion battery exploiting layered oxide cathode, graphite anode and glyme-based electrolyte. *Journal of Power Sources* 310: 26–31.

43 Palaniselvam, T., Babu, B., Moon, H. et al. (2021). Tin-containing graphite for sodium-ion batteries and hybrid capacitors. *Batteries & Supercaps* 4: 173–182.

44 (a) Laziz, N.A., Abou-Rjeily, J., Darwiche, A. et al. (2018). Li-and Na-ion storage performance of natural graphite via simple flotation process. *Journal of Electrochemical Science and Technology* 9: 320–329. (b) Liu, K., Yang, S., Luo, L. et al. (2020). From spent graphite to recycle graphite anode for high-performance lithium ion batteries and sodium ion batteries. *Electrochimica Acta* 356: 136856.

45 Goktas, M., Bolli, C., Berg, E.J. et al. (2018). Graphite as cointercalation electrode for sodium-ion batteries: electrode dynamics and the missing solid electrolyte interphase (SEI). *Advanced Energy Materials* 8: 1702724.

46 Escher, I., Kravets, Y., Ferrero, G.A. et al. (2021). Strategies for alleviating electrode expansion of graphite electrodes in sodium-ion batteries followed by in situ electrochemical dilatometry. *Energy Technology* 9: 2000880.

47 Escher, I., Hahn, M., Ferrero, G.A., and Adelhelm, P. (2022). A practical guide for using electrochemical dilatometry as operando tool in battery and supercapacitor research. *Energy Technology* 2101120.

48 Goktas, M., Bolli, C., Buchheim, J. et al. (2019). Stable and unstable diglyme-based electrolytes for batteries with sodium or graphite as electrode. *Applied Materials and Interfaces* 11: 32844–32855.

49 Zhang, H., Li, Z., Xu, W. et al. (2018). Pillared graphite anodes for reversible sodiation. *Nanotechnology* 29: 325402.

50 Guan, Z., Shen, X., Yu, R. et al. (2016). Chemical intercalation of solvated sodium ions in graphite. *Electrochimica Acta* 222: 1365–1370.

51 Xu, K. (2014). Electrolytes and interphases in Li-ion batteries and beyond. *Chemical Reviews* 114: 11503–11618.

52 Maibach, J., Jeschull, F., Brandell, D. et al. (2017). Surface layer evolution on graphite during electrochemical sodium-tetraglyme cointercalation. *ACS Applied Materials & Interfaces* 9: 12373–12381.

53 Wang, Z., Yang, H., Liu, Y. et al. (2020). Analysis of the stable interphase responsible for the excellent electrochemical performance of graphite electrodes in sodium-ion batteries. *Small* 16: 2003268.

54 Kim, H., Lim, K., Yoon, G. et al. (2017). Exploiting lithium–ether co-intercalation in graphite for high-power lithium-ion batteries. *Advanced Energy Materials* 7: 1700418.

55 Nie, M., Chalasani, D., Abraham, D.P. et al. (2013). Lithium ion battery graphite solid electrolyte interphase revealed by microscopy and spectroscopy. *The Journal of Physical Chemistry C* 117: 1257–1267.

56 Westman, K., Dugas, R., Jankowski, P. et al. (2018). Diglyme based electrolytes for sodium-ion batteries. *ACS Applied Energy Materials* 1: 2671–2680.

57 (a) Ellis, L.D., Hatchard, T.D., and Obrovac, M.N. (2012). Reversible insertion of sodium in tin. *Journal of The Electrochemical Society* 159: A1801–A1805. (b) Li, Z., Ding, J., and Mitlin, D. (2015). Tin and tin compounds for sodium ion battery anodes: phase transformations and performance. *Accounts of Chemical Research* 48: 1657–1665.

58 Chevrier, V.L. and Ceder, G. (2011). Challenges for Na-ion negative electrodes. *Journal of The Electrochemical Society* 158: A1011.

59 Palaniselvam, T., Goktas, M., Anothumakkool, B. et al. (2019). Sodium storage and electrode dynamics of tin-carbon composite electrodes from bulk precursors for sodium-ion batteries. *Advanced Functional Materials* 29: 1900790.